A case of an intense anticyclonic eddy in the Balearic Sea (western Mediterranean)

Ananda Pascual,[1] Bruno Buongiorno Nardelli,[2] Gilles Larnicol,[3] Mikhail Emelianov,[4] and Damià Gomis,[1]

Received 10 April 2001; revised 3 December 2001; accepted 25 February 2002; published 6 November 2002.

[1] Sea surface topography from TOPEX/Poseidon and ERS satellites, SST images derived from advanced very high resolution radiometer (AVHRR) sensors, and conductivity-temperature-depth (CTD) data collected during an oceanographic survey are examined to investigate an intense mesoscale anticyclonic eddy observed at the northern boundary of the Balearic Sea (western Mediterranean). This eddy, which constitutes the strongest signal detected in the Balearic basin since altimetric data are available, appeared in September 1998 to the northwest of Menorca Island and remained almost in the same location until its disappearance in March 1999. The paper focuses mainly on identifying the conditions that led to the eddy formation and on the description of its evolution and sudden disappearance. Derived variables such as geostrophic velocity or vorticity are computed to complement the hydrographic and dynamical information provided by observed variables. Also, meteorological data are examined related to the main hypothesis made for the origin of the eddy. *INDEX TERMS:* 4223 Oceanography: General: Descriptive and regional oceanography; 4275 Oceanography: General: Remote sensing and electromagnetic processes (0689); 4283 Oceanography: General: Water masses; 4520 Oceanography: Physical: Eddies and mesoscale processes; 4536 Oceanography: Physical: Hydrography; *KEYWORDS:* eddies, Balearic Sea, Mediterranean Sea, altimetry, AVHRR, hydrography

Citation: Pascual, A., B. Buongiorno Nardelli, G. Larnicol, M. Emelianov, and D. Gomis, A case of an intense anticyclonic eddy in the Balearic Sea (western Mediterranean), *J. Geophys. Res.*, *107*(C11), 3183, doi:10.1029/2001JC000913, 2002.

1. Introduction

[2] The Balearic Sea is a subbasin of the western Mediterranean located between the Iberian Peninsula and the Balearic Islands (Figure 1). It is limited to the north by the Liguro-Provençal Basin, characterized by strong atmospheric forcings [*MEDOC Group*, 1970], and to the south by the Algerian Basin dominated by intense mesoscale eddies and their interactions with the unstable Algerian current [*Millot*, 1991]. Consequently, the Balearic Basin acts as a transition region between two different regimes, playing a key role in the western Mediterranean general circulation.

[3] The major aspects of the dynamics and the typical water mass structure in the Balearic Sea are fairly well known and have been described by several authors [e.g., *Font et al.*, 1988; *Pinot et al.*, 1995; *López-Jurado et al.*, 1996; *Millot*, 1999]. The circulation is controlled by two permanent density fronts: the Catalan front over the Iberian Peninsula slope and the Balearic front, located over the insular slope (Figure 2). The Catalan front is a shelf/slope front that separates old Atlantic Water (AW) (Water mass acronyms in this paper follow the recent recommendations of the Round Table on Mediterranean Water Mass Acronyms, 36th CIESM Congress, Monaco, 2001. (http://ciesm.org/events/RT5-WaterMassAcronyms.pdf).), in the center of the Balearic Sea, from the less dense water transported by the Northern current, which is also old AW but fed in the Gulf of Lions and Catalan shelves by fresh continental water. The Northern current flows southwards, along the continental slope, until it either exits the basin through the Ibiza channel or recirculates cyclonically over the islands slope forming the Balearic current. This latter current is also fed by warm and fresh recent AW coming from the Algerian Basin through the Mallorca and Ibiza channels. Thus, the Balearic front separates old AW, present in the middle of the basin, from the less dense water transported by the Balearic current.

[4] Previous in situ and satellite imagery studies [*La Violette et al.*, 1990; *Tintoré et al.*, 1990; *Millot*, 1991; *López García et al.*, 1994; *Pinot et al.*, 1994; *Font et al.*, 1995] had already revealed the significant variability of the general circulation in the Balearic Sea in a wide range of spatial and temporal scales. Even in this context, 1998 was an exceptional year. First, because it accounted for the highest value of Sea Level Variability (SLV) of the seven

[1]Institut Mediterrani d'Estuidis Avançats, IMEDEA (CSIC-UIB), Mallorca, Spain.
[2]Istituto di scienze dell'atmosfera e del clima-sezione di Roma, Rome, Italy.
[3]CLS Space Oceanography Division, Toulouse, France.
[4]Centre Mediterrani d'Investigacions Marines i Ambientals, CMIMA (CSIC), Barcelona, Spain.

0148-0227/02/2001JC000913

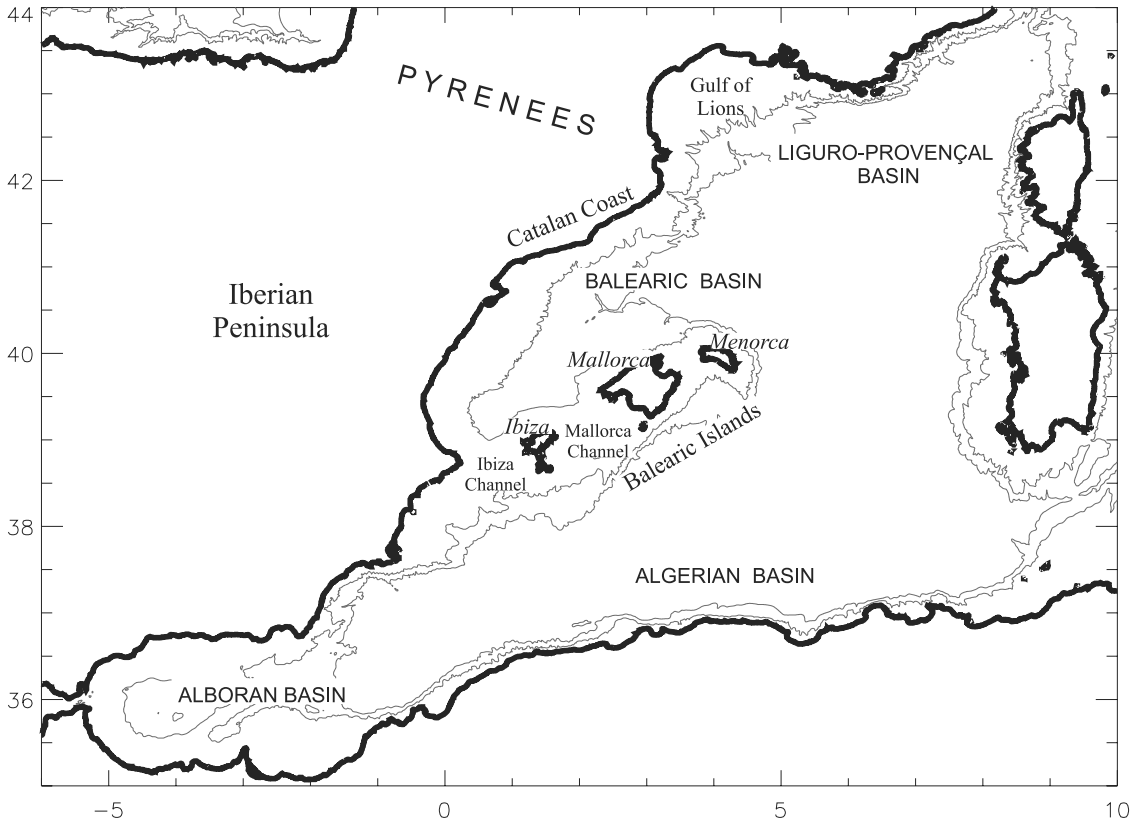

Figure 1. Location of the study area in the western Mediterranean. The 1000 and 2000 m isobaths are plotted.

years period (1993–1999) of altimetric data analyzed by *Larnicol et al.* [2002]. Second, because most of this variability was associated with a single mesoscale anticyclone observed to the northwest of Menorca Island. This eddy constituted a very singular event for what concerns its intensity (heights of more than 30 cm with associated velocities of up to 60–70 cm/s), persistence (about 6 months) and spatial dimension (about 90–100 km diameter). Moreover, it produced a reversal of the usual cyclonic circulation in the Balearic basin.

[5] The origin, development and decay of this eddy are the subjects of the present study. More precisely, the paper will focus on determining the conditions that led to the eddy formation, on the description of its evolution, and on making some hypotheses for its sudden disappearance. Results will base on a combination of satellite and in situ oceanographic data, as well as on some meteorological data related to crucial hypotheses made throughout the paper.

[6] The presentation is organized as follows: after a brief description of the data sets (section 2), section 3 will be entirely devoted to present the results. The origin of the eddy will be described in section 3.1. In section 3.2, the mature phase of the anticyclone will be analyzed, focusing first on the evolution of the structure as observed from satellite data and then on its hydrological and dynamical characteristics inferred from in situ data. The decay will be reported in section 3.3. In section 4, results will be discussed paying

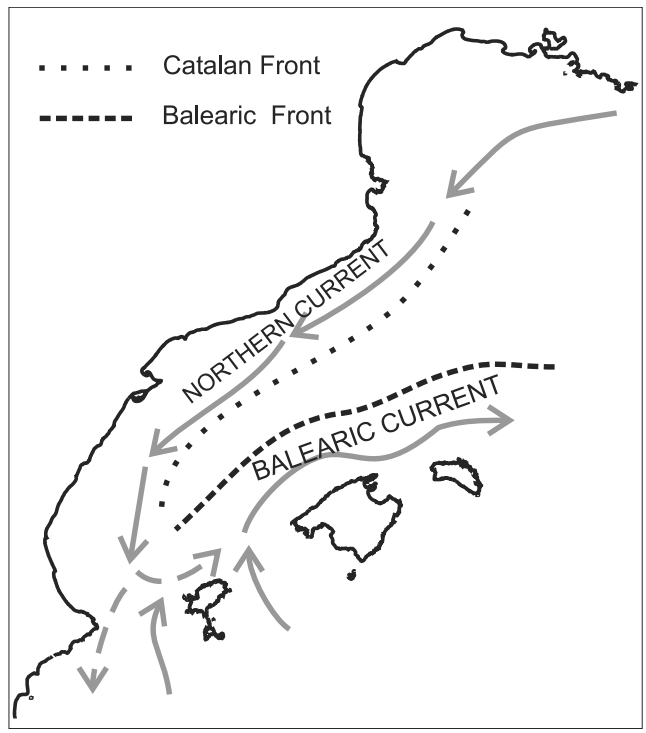

Figure 2. Main fronts and currents in the Balearic Sea.

special attention to the physics underlying the occurrence of this event, and conclusions outlined.

2. Data Sets

[7] The complementary characteristics of satellite and in situ data proved to be very useful for this case study. Oceanographic cruise data provide an accurate, spatially dense 3D view, but it is limited to a certain region and it can hardly be repeated in time. Conversely, advanced very high resolution radiometer (AVHRR) sensors on NOAA satellites provide a high frequency, spatially dense coverage that is essential for monitoring mesoscale features in the ocean, but they only measure surface temperature. Altimetry provides information that is somehow in between the two previous sources. On the one hand, the surface circulation can be estimated from sea surface heights, and, making some assumptions about the baroclinic nature of the flow (i.e., that the absolute velocity vanishes at some reference level), also some considerations about the 3D density field can be inferred (see section 3.2.3). On the other hand, altimetry observations have a temporal and spatial resolution lower than AVHRR data. The three specific data sets used in this work are briefly described in the following.

[8] Sea Surface Temperature (SST) images were acquired by the HRPT station of the Istituto di Fisica dell'Atmosfera (Rome, Italy) from the AVHRR sensors mounted on NOAA 12 and NOAA 14. The data were processed using the DSP software developed at Miami University. The algorithm adopted here to compute SST was based on a *split window* technique that allows the correction of atmospheric attenuation using the brightness temperature of two infrared channels [*MacClain et al.*, 1985].

[9] Altimetry data used for this study include along-track TOPEX/Poseidon (T/P) data as well as a sequence of maps of combined T/P and ERS-1/2 data. The processing of both data sets first consisted of the usual geophysical corrections [*Le Traon and Ogor*, 1998]. The data were then resampled every 14 km along the tracks using cubic splines. In order to eliminate geoid signals, Sea Level Anomaly (SLA) were constructed by removing a 4 year mean (1993–1996). Next, the measurement noise was reduced by filtering SLA with a 35 km median filter and a Lanczos filter with a cutoff wavelength of 42 km. To build up the maps, along-track data were optimally interpolated every 10 days on a $0.2^\circ \times 0.2^\circ$ grid using an improved objective analysis [*Le Traon et al.*, 1998]. Statistical errors associated with the interpolation process are shown for the study region in Figure 3.

[10] The cross-track component of the geostrophic velocity field can be obtained by differencing along-track SLA data. In principle, the geostrophic approximation does not hold in presence of strong curvature, as it neglects the centripetal force from the momentum balance. For an anticyclone (the case presented here), this yields to an underestimation of the actual velocity field. The importance of cyclostrophic acceleration relative to the Coriolis acceleration has been estimated by *Gomis et al.* [2001] obtaining a ratio of about 0.17 in the western Alboran gyre, and similar results were obtained by *Benzohra and Millot* [1995] for an Algerian eddy. Thus, the underestimation of the actual velocity field for an eddy of similar characteristics to the one described here would be of about 20%, which is of the order of altimeter accuracy.

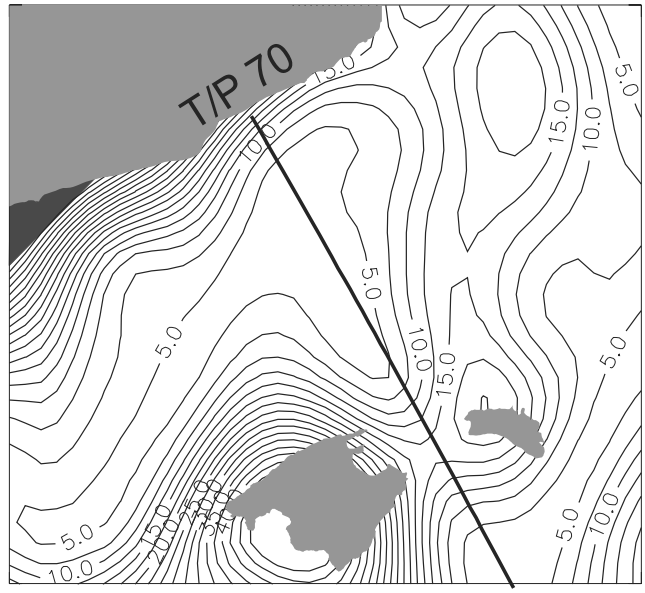

Figure 3. Statistical error map associated with the interpolation analysis of SLA along-track data. The error is expressed in percentage relative to the signal. T/P track 70 (particularly relevant for this study) is also indicated with a solid line.

[11] In situ data were collected during the *Hivern-99* oceanographic cruise, carried out on board R/V *Garcia del Cid* from 20 February to 15 March 1999. A total of 84 surface-to-bottom conductivity-temperature-depth (CTD) casts were obtained and were preprocessed using standard software. Due to bad weather, the cruise had several interruptions. For temporal coherence, the data analysis restricted to a subset of transects (shown in Figure 9) that were sampled almost synoptically (between 25 and 28 February) and, separately, to a few profiles collected the first days of March. Dynamic height profiles were computed with a reference level of 1000 m.

3. Results

3.1. Origin of the Eddy

[12] The origin of the eddy was mainly traced from a sequence of SST images covering the period from June 1998 to the end of September 1998. Using single satellite passes instead of weekly or monthly averages allowed to monitor the rapid evolution of small features resulting from instabilities of the main surface flow. A selection of the clearest SST images is presented in Figure 4, the intervals being shorter when following the evolution of particular mesoscale features and longer when the surface pattern remained almost stationary.

[13] The image of 18 June 1998 (Figure 4a) shows the typical situation characterizing the surface circulation in the northwestern Mediterranean. The northern part of the Balearic Basin is occupied by old AW carried southwestward by the Northern current and cooled all year round by the strong Mistral wind in the Gulf of Lions. This cold water splits into two branches around 3°E. The first branch deviates to the

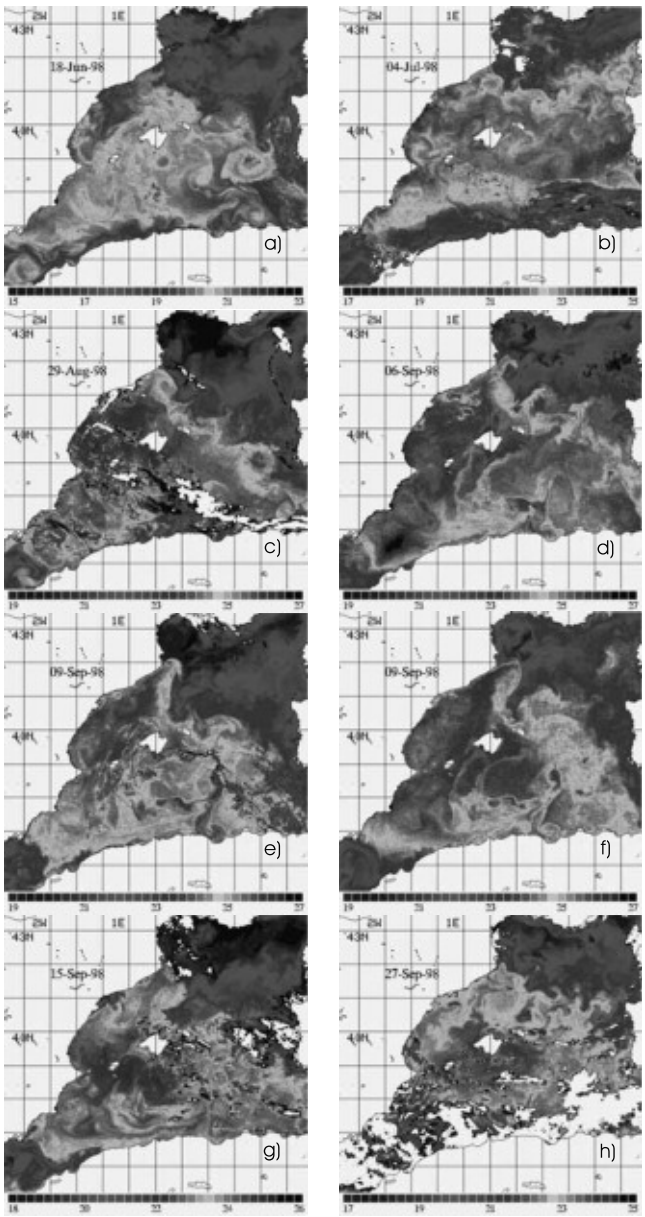

Figure 4. Sequence of AVHRR images of the western Mediterranean. Longitude labels correspond to the ticks on the left. See color version of this figure at back of this issue.

east-southeast and constitutes the main contribution to the cyclonic circulation of the Medoc region. The second, slightly less cold branch continues along the Iberian shores. Along the western slope of the Balearic Islands, a tongue of warm water coming from the Ibiza and Mallorca channels is the thermal signature of the Balearic current. In the lower part of the image, the entrance of the cooler recent AW from the Alboran gyres is well identified. As this water flows to the east along the Algerian coast, it is gradually warmed and mixed with the relatively warmer resident waters. Several instabilities with different length scales modulate the flow, culminating in the large anticyclones visible in the central part of the Algerian Basin.

[14] On 4 July (Figure 4b) the Northern and Balearic currents are no longer apparent because of the intense heating of the sea surface. In fact, climatological studies [*López García et al.*, 1994] have shown that in summer the Catalan front does not reach the surface, whereas the surface signature of the Balearic front is still evident in the salinity field but not in the temperature field. Conversely, a new thermal front, referred to as the Pyrenees front, is visible perpendicular to the Catalan coast. This results from the shadowing effect of the Pyrenees over the Mistral jet, which cools the sea surface and induces surface mixing (i.e., counteracts the seasonal stratification associated with solar heating). Namely, the Pyrenees deviate the Mistral in such a way that its cooling effect is restricted to the Gulf of Lions. The Pyrenees front is therefore a very shallow structure separating stratified and nonstratified surface layers.

[15] A Mistral event occurred by the end of August, as observed in wind and atmospheric pressure data (J. Campins, personal communication, 2001) (Figure 6a). This event reflected also in the SST (image of 29 August, Figure 4c) with a marked decrease of the temperature in the Gulf of Lions. Figure 4c also shows a northeastward tongue of warm water along the Catalan coast but wind stress prevented it from progressing northward. Conversely, during the first week of September, the absence of Mistral winds (Figures 6b and 6c) allowed the northward advance of the flow. In the SST the latter appears as a thin vein with a mushroom structure protruding in the Gulf of Lions (Figure 4d, 6 September).

[16] Just after this warm intrusion in the Gulf of Lions, two strong Mistral events were registered between 8 and 12 September (see Figure 6d as a sample). They are thought to be the main responsible for the transmission of anticyclonic vorticity to the northern edge of the warmer tongue, which is apparent in SST images of 9 September (Figures 4e at 02:40 h and 4f at 17:45 h). In the image of 15 September (Figure 4g), well after the storms, the Gulf of Lions appears much cooler and, most important, the warm tongue has disappeared forming an anticyclonic spiraling. The mechanism for the transmission of anticyclonic vorticity is the negative curl associated to the shear of the Mistral downstream of the Pyrenees (similar features in the Mediterranean are the Ierapetra gyre and the Tyrrenian eddies [see *Horton et al.*, 1994]). By 27 September (Figure 4h) the eddy is already quite evident as a sort of subbasin-scale gyre of about 100 km radius centered at 3.5°E, 41°N. A narrow filament seems to continue feeding the eddy with warm water coming from the Mallorca channel.

[17] The birth of the eddy was also monitored from altimetry data. It was a fortunate coincidence that T/P track 70 (see Figure 3) crossed almost exactly the eddy center (despite the formation of filaments and other changes in its shape) and that it remained almost in the same location for most of its life. Hence, T/P provided a suitable continuous (10 day spaced) sampling of this structure.

[18] Figure 5 shows the along track geostrophic velocity derived for T/P cycles 219 (27 August) and 221 (16 September); cycle 220 is absent for this particular track. By the end of August a northeastward current along the Catalan coast, with velocities of about 30 cm/s, is depicted and it is coherent with Figure 4c. On 16 September altimetry already reports an intense anticyclonic circulation, showing a symmetrical pattern between northern and southern fluxes (>60 cm/s). The radius of the eddy (estimated

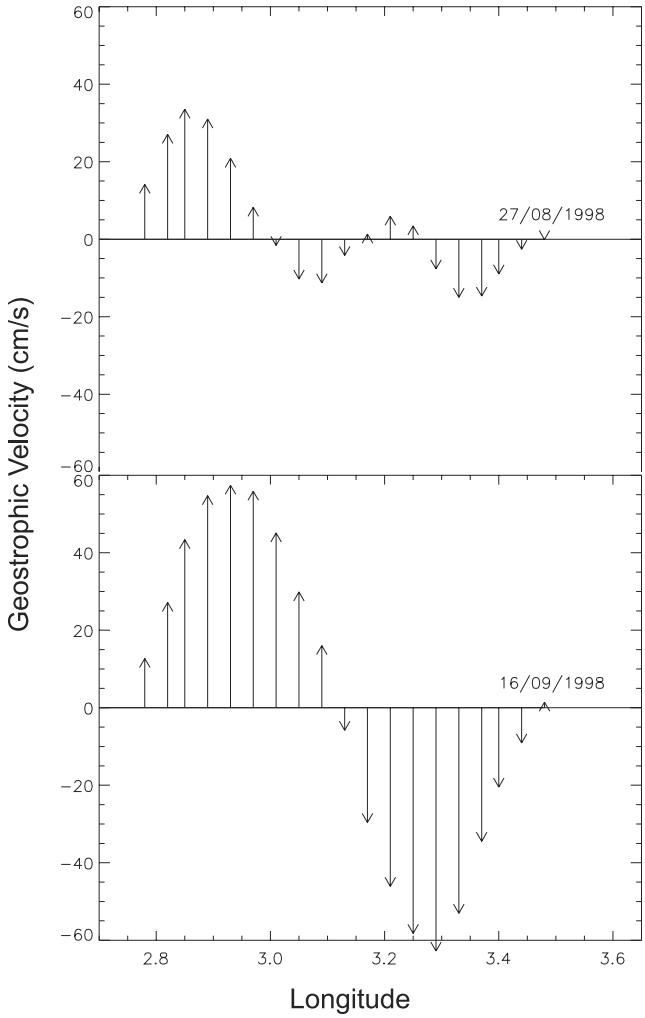

Figure 5. Cross-track geostrophic velocities inferred from T/P along-track data for 27 August 1998 and 16 September 1998. The *x* axis is longitude, the Catalan coast being on the left side of the figure and the Balearic coast being on the right side. Positive values mean northeastward flow.

from track points resampled every 14 km) is about 100 km, i.e. of the same dimension as seen in the SST images (Figures 4g and 4h).

3.2. Life of the Eddy

3.2.1. Temporal Evolution at Surface From Satellite Data

[19] The description of the evolution of the eddy after its formation will focus on the northern part of the Balearic Sea, where the anticyclonic eddy remained for most of its life (Figure 7). Cross-track geostrophic velocities derived from the altimeter cycles closer to the date of every selected image have been plotted onto the SST distributions.

[20] By 13 October (Figure 7a), the anticyclone became smaller (less than 50 km radius) and moved toward Menorca Island. The Pyrenees front was still present limited by the northern edge of the eddy. The latter showed an irregular shape, with two meanders and a sort of warm jet around 41°N starting to wrap around the cooler water from the Gulf of Lions. Altimetry reports a clear anticyclonic circulation associated with the eddy, with values of up to 40 cm/s on the side of the Balearic Islands and smaller on the other side. However, the center of the eddy SST pattern does not exactly coincide with the position of the T/P track, so that actual velocities could be larger than estimated ones.

[21] In the SST image of 9 November (Figure 7b), the whole basin is displayed, in order to show how the eddy is still fed by warm water entering through the Balearic channels. More to the north, surface cooling goes on, and the Northern current is again visible in the image. The eddy core temperature is of about 20°C, while the water along the Catalan coast attains around 18°C. In this image the eddy appears almost elliptic, with two filaments detaching from the extremes of the major axis. This observation is particularly interesting, as detailed studies on the evolution of isolated elliptical vortexes [*Melander et al.*, 1987] have demonstrated that filament generation is a mechanism by which vortexes are relaxed toward an axisymmetric shape.

[22] This has apparently happened by 13 December (Figure 7c), when the eddy is almost round and no filaments can be identified, even if a spiraling tongue of warm water from the northern part of the anticyclone is clearly advected by the Northern current along the Iberian Peninsula. At this time, maximum cross-track velocities reached almost 70 cm/s and the center of the eddy, as identified in the SST images, is exactly located where the velocity vanishes. By the beginning of January (Figure 7d) the Pyrenees front appears as a straight latitudinal structure along 41°N, separating the cold waters of the northern part of the basin from the 100 km wide warm anticyclone. Maximum velocities of up to 60–70 cm/s are found at the boundaries of the eddy.

[23] In the next image (15 January, Figure 7e), the northern boundary of the anticyclone is shown to be distorted by a cold water jet. Part of the warm water that constituted the eddy is pushed to the east and then to the south. The presence of Menorca Island seems to prevent this water from being kept within the eddy structure. The altimetric signature of the eddy has weakened and its intensity and shape both agree with the SST pattern. A further pinching off is observed 5 days later (not shown), caused by an intense cold flow from the Gulf of Lions turning west of Menorca.

[24] By the 24 January, the eddy has evolved toward a smaller structure (Figure 7f). At this stage it is again characterized by an elongated, almost elliptic shape, with some spiraling filaments wrapping around the eddy's core. Also altimetry data suggest that the eddy size had reduced and surface slopes had decreased (maximum associated speeds went down to about 20 cm/s on the Catalan coast), even taking into account that the center of the eddy is located considerably to the east of the T/P track.

[25] The development of filaments proves again as a very effective mechanism to transform the eddy in an axisymmetric structure. Hence, about 10 days later (5 February, Figure 7g) the anticyclone has acquired an almost perfect round shape centered at 41°N, 2.2°E with a radius of around 40 km. The same size and position of the eddy is deduced from altimetry, with maximum velocities of about 40 cm/s.

[26] In the following weeks, the Northern current has the aspect of an intrusion pulling the eddy southeastward (25 February, Figure 7h). It is worth noting that despite the eddy

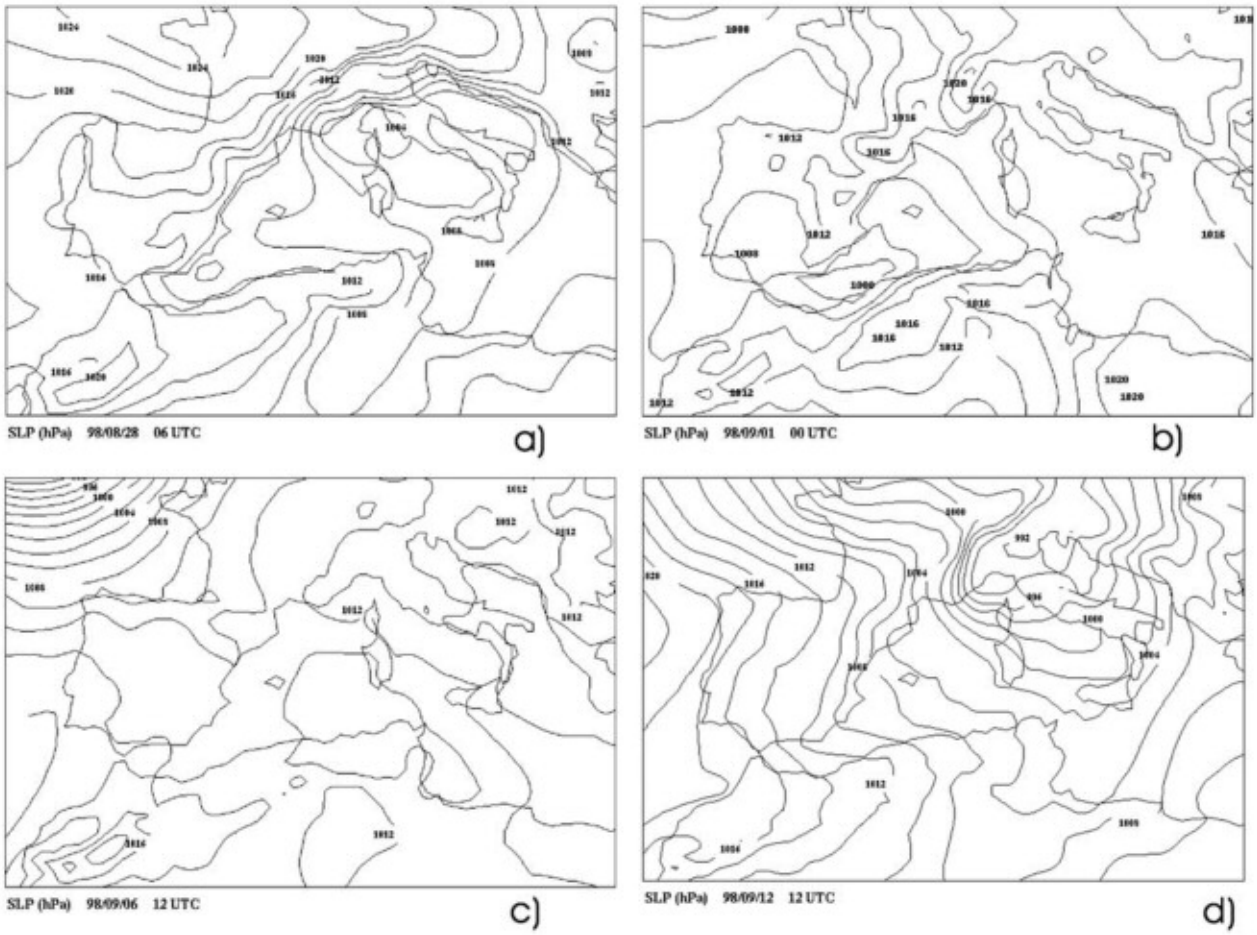

Figure 6. Maps of Sea Level Pressure (SLP) from the HIRLAM-INM model. Resolution is 0.5°, and isobars are plotted every 2 mbar. During Mistral events, actual winds in the sea are usually stronger than those depicted from the SLP maps of the HIRLAM model, due to the lack of observations in the ocean.

has displaced to the east of the T/P track 70 (as inferred from SST imagery), SLA still reports a very clear anticyclonic signature. A reason for that could be that SLA data are from 21 February, while the SST image is from 25 February (this implying that the eddy would have started to drift eastward after the 21st). The last image previous to the decay of the eddy corresponds to 2 March (Figure 7i). There it appears as an elongated eddy and is found considerably to the east (between 2° and 3.5°E). Altimetric measurements of the next day also reveal a reduction of the velocity field, although this could partially due to the displacement of the eddy with respect to the satellite ground track.

[27] A complementary way of describing the eddy's life and evolution is by SLA maps, which give a more complete 2D view of the surface circulation. Figure 8 shows a set of maps corresponding to dates close to the SST images of Figure 7. In general terms, the shape of the anticyclonic eddy depicted in the maps is quite coherent with AVHRR images. Thus, the asymmetric meandering shape exhibited by the eddy on October is well apparent in the corresponding SST image and altimetry map (Figures 7a and 8a). So they are the elongated shape and strong gradients on its eastern side observed in December (Figures 7c and 8b). By the beginning of January, SST imagery revealed a southwards shift of the eddy, with slightly stronger gradients on its northern border (Figure 3d). A similar behavior and pattern are observed in the corresponding altimetry maps (Figure 4c). The reduction of the size and intensity of the eddy detected by the second half of January, as well as its displacement to the north, is also seen in both Figures 7f and 8d. Even the evidences for a secondary, small anticyclonic eddy located to the northeast of Menorca are in good agreement. But the eastward shift shown in Figure 7h is not captured by the altimetric maps (Figure 8e) probably because of the same reason that it was not apparent in the along-track data. Finally, in Figure 8f the anticyclonic signature is not visible any more (the decay of the eddy will be commented in more detail in section 3.3).

3.2.2. Hydrographic Structure of the Eddy in February 1999

[28] By the end of February 1999, an oceanographic cruise named as *Hivern-99* was carried out in the region as part of a routine sampling strategy. Because the cruise was not aimed to study the eddy, this was not sampled in an optimal way. Nevertheless, the hydrographic data collected during the cruise turned to be very useful to identify the water masses constituting the eddy, as well as its deep structure.

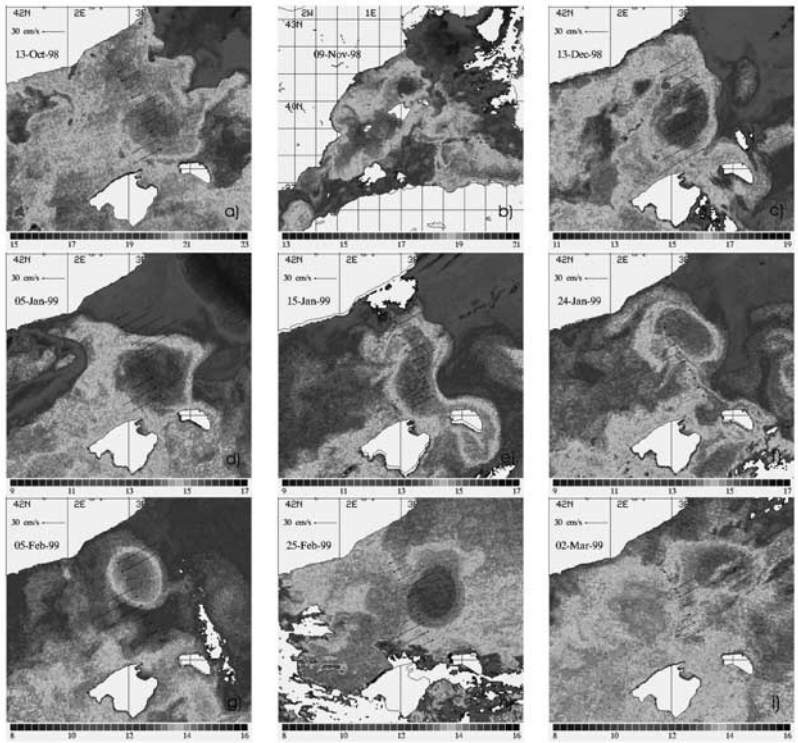

Figure 7. Sequence of AVHRR images of the Balearic Sea. Vectors of cross-track geostrophic velocities inferred from T/P along-track data have been overplotted. See color version of this figure at back of this issue.

[29] A first overall perspective of the eddy is given by the surface dynamic height field, obtained by the interpolation the data collected during 25–28 February (Figure 9). The center of the eddy seems to be located within the sampled region, at about 3.2°E 40.7°N (station 38, and almost in the middle of the basin), and the observed irregular shape is quite coherent with the SLA and SST patterns of 24 and 25 February, respectively. For a view of the deep structure (down to 1000 m) transects T1 and T2 have been selected, since they are the closest to T/P track 70 and, in some way complementary: T2 runs almost across the center of the eddy, but only provides information on its northeastern side; T1 offers a view of the complete southern edge of the eddy.

[30] Both transects reveal that the core of the eddy was characterized by high temperature (Figures 10a and 11a) and low salinity values (Figures 10b and 11b). Maximum surface temperatures of 14.2° are found on station 38, and are consistent with the AVHRR images of the same days (Figure 7h). Concerning salinity values at the upper layers, they are of 37.7–37.8 over stations 22–26 on transect T1 and on transect T2 over stations 37 and 38. Therefore, according to the TS surface values, we can confirm that the

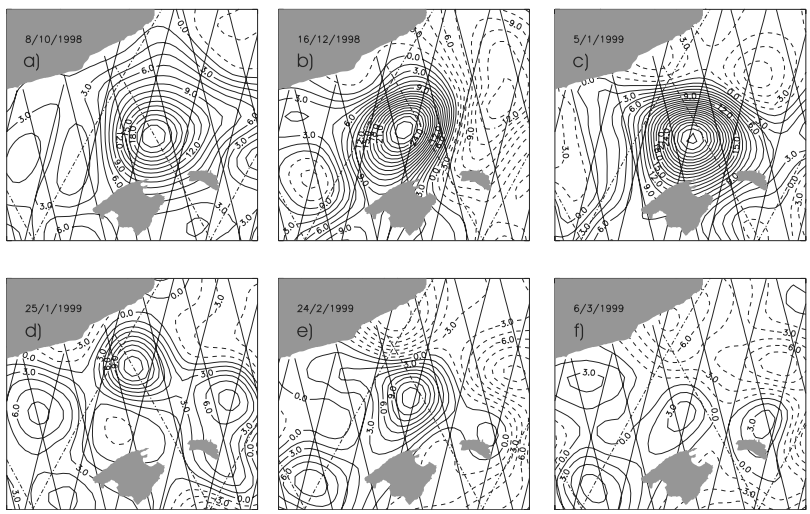

Figure 8. Sequence of SLA maps derived from T/P-ERS-2 data.

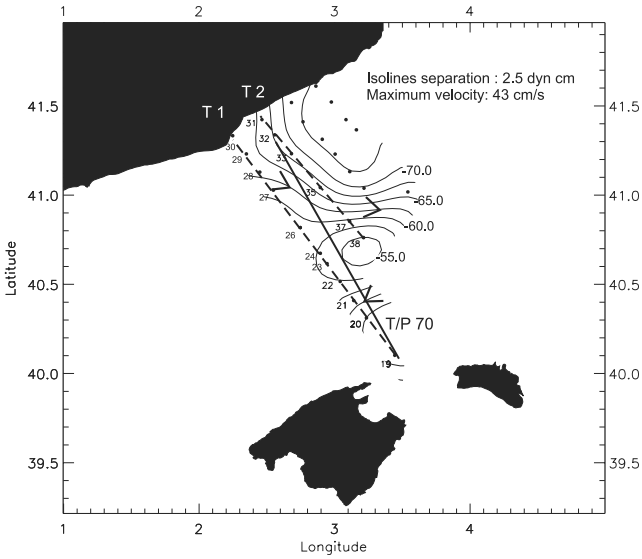

Figure 9. Station distribution of the *Hivern-99* cruise, with selected transects T1 and T2 (dashed lines). T/P track 70 is indicated with a solid line. The dynamic height field at 10 m (reference level 1000 m) is overplotted.

eddy was formed by recent AW, that may have crossed the Balearic channels coming from the Algerian Basin. However, a salinity value of 37.7–37.8 also indicates that there has been some mixing with the saltier waters of the surroundings during the life of the eddy, because recent AW that usually penetrates the Balearic channels have salinities lower than 37.5 [*López-Jurado et al.*, 1996].

[31] It is worth noting that in this case study, the lowest surface salinity values (corresponding to the eddy's core) are found almost in the middle of the Balearic Sea. Conversely, in a typical situation, the center of the basin would be occupied by the saltiest water mass, i.e. old AW. Recent AW would be confined to a shallow layer located near the Balearic Islands (at the eastern edge of T1) and old AW mixed with fresh waters would be present on the Catalan side [*López-Jurado et al.*, 1996].

[32] Below recent AW, some subsurface cores of Western Mediterranean Intermediate Waters (WIW) can also be distinguished between 200 and 300 m, characterized by temperatures below 13°C (Figures 10a and 11a, dashed isolines). Levantine Intermediate Waters (LIW) are detected at intermediate depths (~600 m), characterized by salinity maxima higher than 38.4 (Figures 10b and 11b, dashed lines). Finally, Western Mediterranean Deep Waters (WMDW) are found in deeper layers specially in T2. However, the presence of these water masses is not anomalous [*López-Jurado et al.*, 1996].

[33] The low salinity and high temperature of the eddy core contribute in the same sense to the buoyancy of the structure (Figures 10c and 11c). Hence, the marked deepening of isopycnals (down to almost 600 m in the center of the eddy, in T2) is in sharp contrast with the smooth dome usually observed in the region. Values for the cross-transect geostrophic velocities (referred to 1000 m) are shown in Figures 10d and 11d. A southwestward flow is depicted on the Balearic side (T1), between stations 19 and 23, with maximum values at surface of more than 25 cm/s. On the other transect (T2), positive (northeastward) values higher than 45 cm/s are found between stations 35 and 38. The asymmetry of maximum values is due to the fact that only transect T2 runs almost across the center of the eddy. Even if the velocities were computed with a reference level of 1000 m, baroclinic velocities below 600 m are negligible (i.e. geostrophic velocities obtained with a reference level of 600 m do not present any noticeable difference).

[34] The presence of the eddy also reflected in the biological environment. In the area occupied by the eddy the phytoplankton community was dominated by prymnesiophytes (including coccolithophorids) and flagellates, species that are typically found in recent AW. To the northwest of the eddy, the dominant group was diatoms, a characteristic species of the saltier Mediterranean waters (M. Estrada, personal communication, 2000).

3.2.3. On the Barotropic/Baroclinic Nature of the Eddy

[35] The fact that geostrophic velocities are robust with respect to the choice of the reference level between 600 and 1000 m implies that below 600 m the baroclinic signal is low. However, geostrophic velocities will still differ from actual velocities in the presence of a barotropic component, which can make some differences, especially for what concerns total transports. The eventual existence of a barotropic component cannot be assessed from hydrographic data alone, but only from independent observations of the velocity field. An alternative is to rely on altimetry, as it has been done by previous authors [e.g., *Gilson et al*, 1998; *Laing and Challenor*, 1999] and, particularly in the Mediterranean by *Buongiorno Nardelli et al.* [1999]. A handicap of the present study is that the hydrographic and altimetric data sets do not exactly coincide either in time or in space (see Figure 9). After carrying out several tests, it was decided to interpolate surface dynamic height onto the T/P track, being aware that the interpolation always involves some kind of smoothing of the raw hydrographic signal. The stations used to carry out the interpolation were performed between the 25 and 28 February, and the closer cycles for T/P track 70 took place on 21 February and 3 March (Figure 12a).

[36] Despite the warnings about the consistency of the two data sets, a good overall agreement was found between the hydrographic and altimetric signals (Figure 12a). This is confirmed by Pearson correlation values, which are 0.98 for the first cycle and 0.80 for the second. Altimetry reports a horizontal dimension of the eddy of about 60 km and an intensity of more than 20 cm, for the first cycle, whereas for the following cycle the signal is smaller (12 cm). The depletion of 8 cm in 10 days is probably due to the displacement of the eddy away from the satellite track rather than to an actual decay. The two cycles also differ in the location of the maximum and in the symmetry of the signal (the second one exhibits higher gradients at the northern side of the track). Dynamic height signal (13 cm) is somehow in between the two altimetric ones, as it could be expected considering the time location of the cruise.

[37] Discrepancies between dynamic height and both cycles of SLA are between ±5 cm and in opposite sense for the two cycles (Figure 12b), as reported previously. Root mean square differences are about 3.4 cm for the first cycle and 3.2 for the second cycle, i.e., of the same order of T/P measurements errors alone [*Tapley et al.*, 1994]. Therefore, even without considering additional error sources (such as interpolation smoothing or the influence of the mean sub-

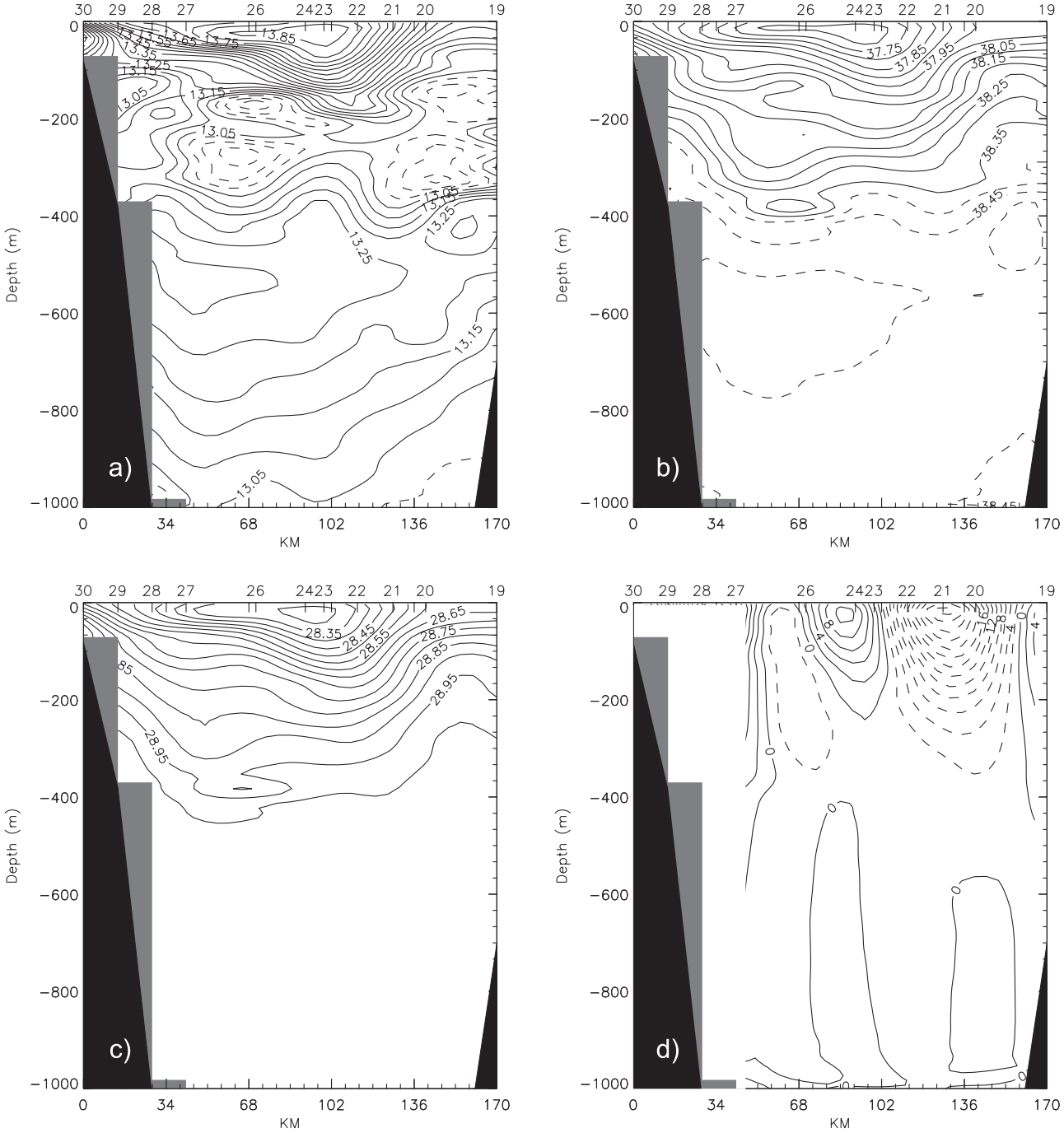

Figure 10. Vertical sections along transect T1: (a) potential temperature (values lower than 13°C are dashed, (b) salinity (values higher than 38.4 are dashed), (c) potential density, and (d) geostrophic velocity computed with a reference level of 1000 m (negative values are dashed and mean southwestward flow). Numbers on the upper part of the figure correspond to stations of Figure 9. Stations not reaching the reference level have been discarded.

tracted to obtain SLA), no reliable evidences for the existence of a barotropic component of the velocity field can be inferred from the differences between hydrographic and altimeter data.

3.3. Decay of the Eddy

[38] From AVHRR images no decay is apparent before 2 March 1999 (Figures 7i and 15a). During the following days (4, 5, and 6 March) severe storms were registered in the region, producing strong winds (see the meteorological map of 4 March, Figure 13) and cloudy weather. The first cloud-free image after the storms (Figure 15b) shows noticeable changes. The Northern current seems to be more intense and wider, especially around the position occupied by the eddy on 2 March. The eddy has been displaced southeastward, now being centered at about 40.5°N and

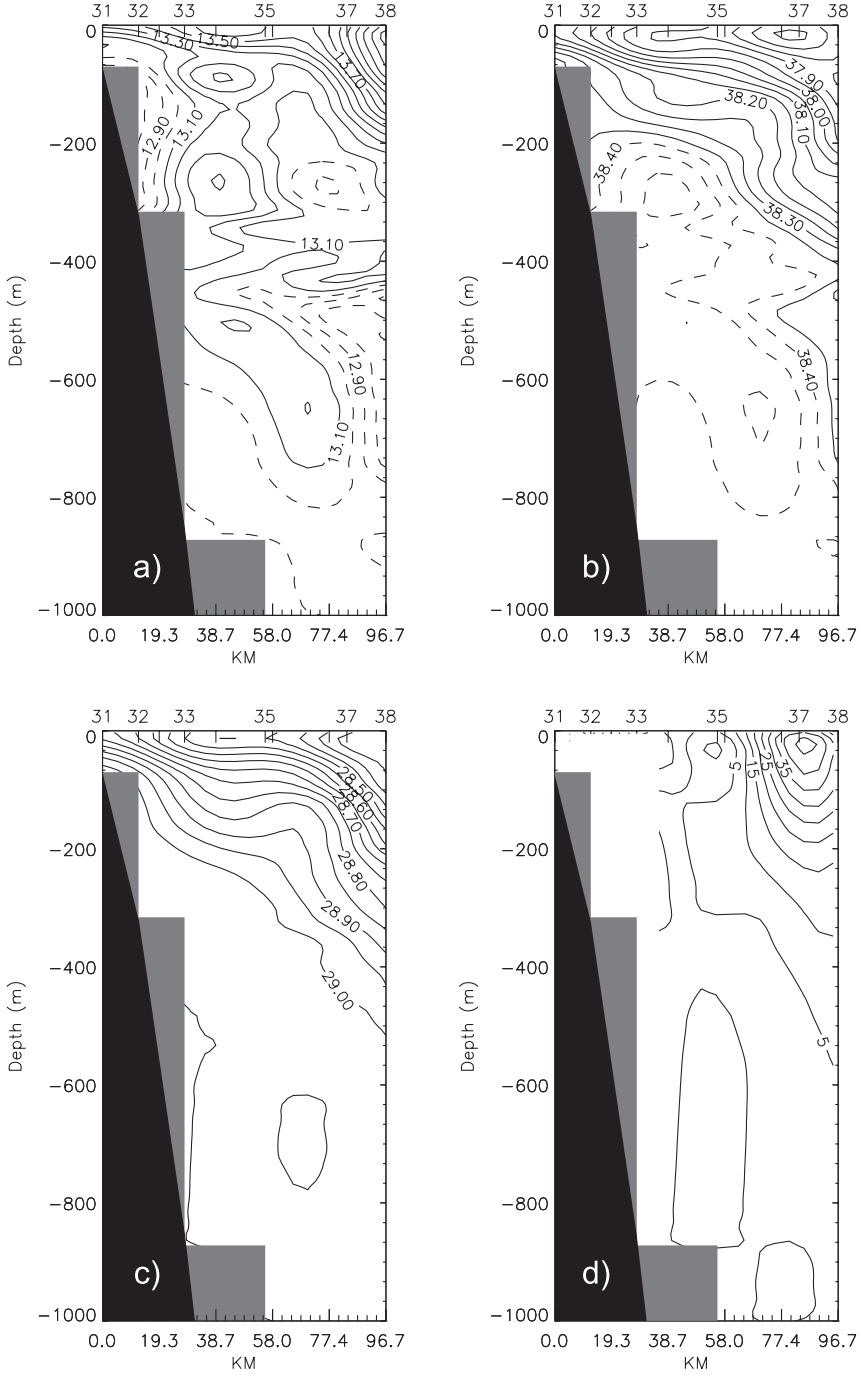

Figure 11. As in Figure 10 but for transect T2.

4.5°E, and shows a more irregular elliptical shape and filaments. At this stage, the Balearic current has the same thermal signature as the anticyclone, since the temperature of the latter's core has decreased by about 1°C (14°C on 7 March, in front of the 15°C observed on 2 March).

[39] The following image (of 9 March) shows how the eddy is loosing coherence and is somehow being incorporated within the Balearic current. On 16 March it is no longer visible, as it had been diluted and/or advected eastward by the Balearic current. The Balearic Basin has thus come back to its typical circulation: the Northern current flows southwestward along the Iberian shores and the Balearic current meanders northeastward along the islands shelf, turning to the east past Menorca.

[40] The replacement of water masses is also evident from the cruise data. Figure 14 shows the temperature and salinity profiles of a CTD station that was repeated two times during the cruise: cast 24 was performed on 25 February (well before the storms) and cast 64 on 7 March (just after the storms). On 25 February the profiles are characteristic of the water mass of the eddy (surface salinities of about 37.7, high temperatures and a sharp thermocline). On 7 March the situation is completely different, presenting higher surface salinity values of 38.1–38.2,

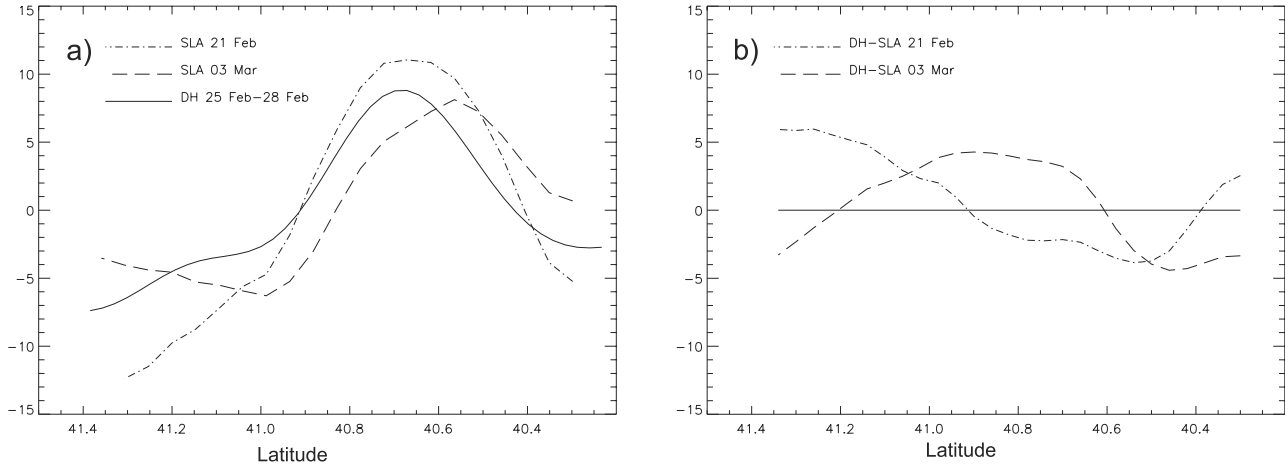

Figure 12. Comparison between altimetry and hydrography along T/P track 70: (a) dynamic height (in dyn cm) at 10 m referred to 1000 m, and SLA (in cm) corresponding to the two cycles closer to the cruise period, and (b) differences between dynamic height and each of the SLA cycles. The CTD data were collected between 25 and 28 February (stations shown in Figure 9), while the closer passages of T/P over track 70 were on 21 February and 3 March.

which indicates that the water mass present in that location was probably advected from the north, as a part of the Northern current. The strong cooling and vertical homogenization down to 200 m are clear effects produced by wind storms.

[41] Finally, when tracking the decay from altimetry maps, the eddy is no longer apparent on the map of 6 March (Figure 8f). Only two small anticyclonic patches (one besides Mallorca and the other besides Menorca) that could be the remaining of the eddy are detected. However, the gradients are very weak (perhaps partly due to the displacement of the eddy to a region in between satellite tracks with a high error due to the interpolation) and nothing can be concluded. No signal was detected outside of the domain.

4. Discussion and Conclusions

[42] The birth, evolution, and decay of an intense anticyclonic eddy detected at the northern boundary of the Balearic Sea from middle September 1998 to middle March 1999 have been studied from a combination of in situ and satellite (AVHRR and altimetry) data. When compared to Mediterranean SLV, the surface anomaly associated with the anticyclone constitutes by itself an exceptional event, as it has already been reported by *Larnicol et al.* [2002]. The abnormality of the event is also clear from Figure 16, which shows the evolution (from September 1997 to October 1999) of the minimum value of geostrophic relative vorticity (computed from SLA maps) observed in the Balearic Sea. While typical minimum values in the basin are of the order of $-1 \cdot 10^{-5}$ s^{-1} ($O(0.1f)$) and are always associated with transient features, the vorticity of the anticyclonic eddy was of the order of $-3 \cdot 10^{-5}$ s^{-1} and lasted for several months.

[43] Regarding the possible mechanisms that yielded the formation of such an exceptional event, there are, in our opinion, three related key points to be considered. Since the core of the eddy was formed by recent AW (as revealed by hydrographic data), this means that this water mass should have entered into the Balearic Sea coming from the Algerian Basin through the Mallorca and Ibiza channels. This constitutes the first point to be contemplated, but it is not possible to determine the amount of AW crossing the channels just from its surface signature of AVHRR images, and sometimes the summer surface warming makes difficult to distinguish old AW from recent AW. Repeated hydrographic measurements carried out by *Pinot et al.* [2002] show that the period from July 1997 to June 1998 was characterized by strong inflows of recent AW through the Mallorca and Ibiza channels. Despite no hydrographic data are available between June 1998 and the formation of the eddy (on September), AVHRR images suggest that the entrance of recent AW would have maintained, if not strengthened, during this period.

[44] Recent AW is thought to be carried by anticyclonic gyres detached from the Algerian current [*Puillat et al.*,

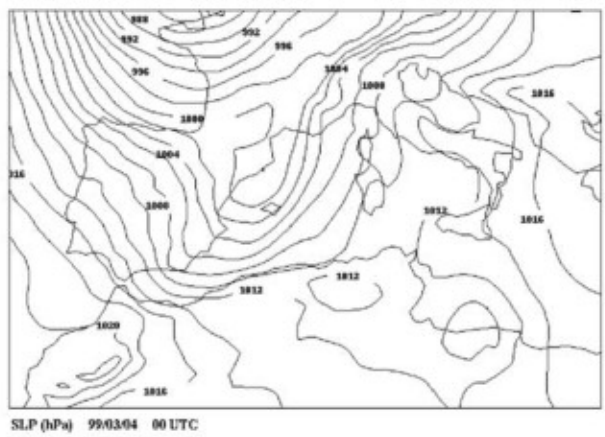

Figure 13. Map of Sea Level Pressure from the HIRLAM-INM model corresponding to 4 March 1999. Resolution is 0.5°, and isobars are plotted every 2 mbar.

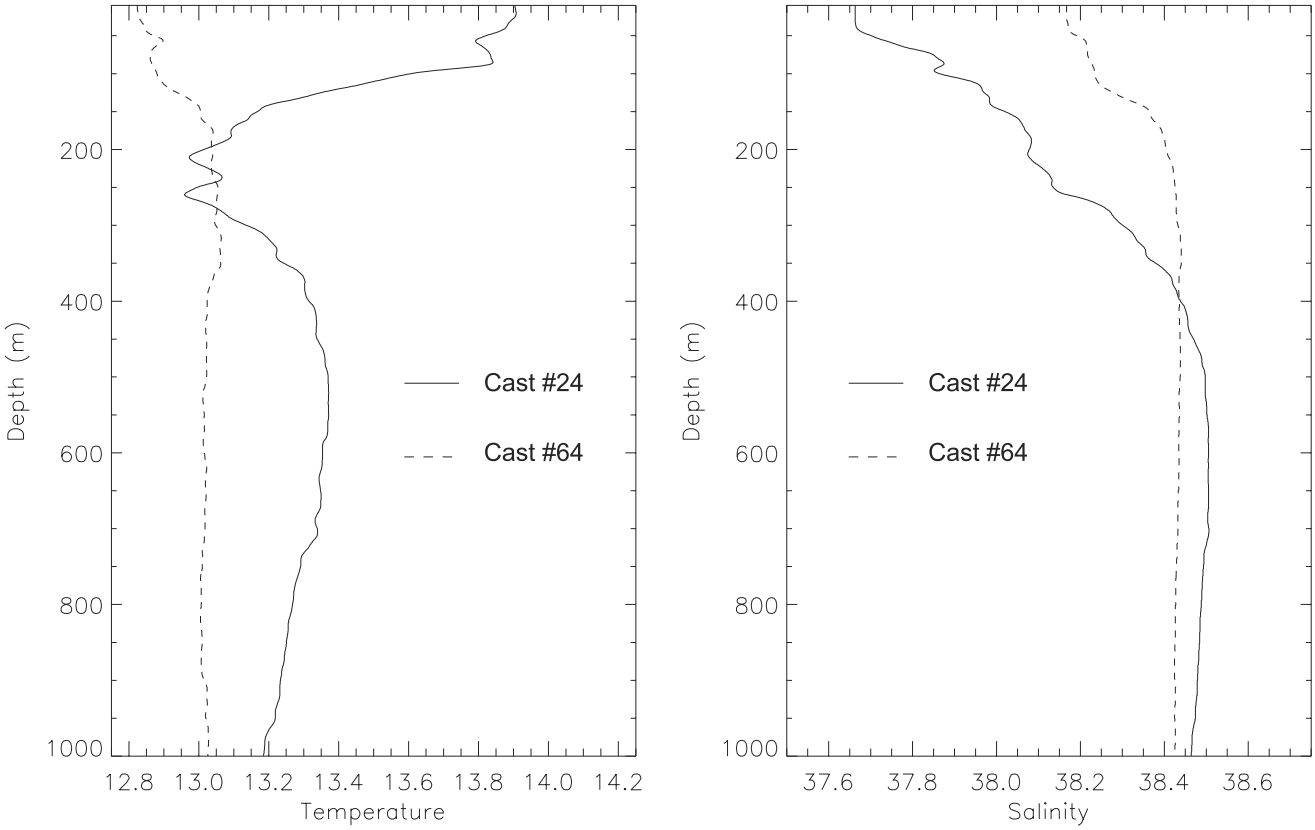

Figure 14. Temperature and salinity profiles for casts 24 and 64 collected on 25 February and 7 March, respectively, in almost the same location (40.7°N, 2.9°E).

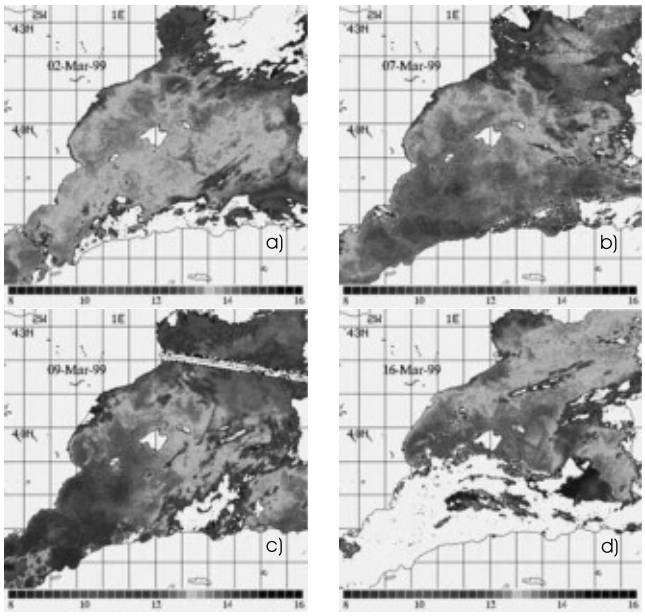

Figure 15. Sequence of AVHRR images of the western Mediterranean. Longitude labels correspond to the ticks on the left. See color version of this figure at back of this issue.

2002; *Ruiz et al.*, 2002]. However, the mechanisms enabling these gyres to reach the Balearic channels or, instead, to migrate elsewhere, are not well established. Winds could play an important role, as it has been suggested by the numerical experiment of *Herbaut et al.* [1997]. This experi-

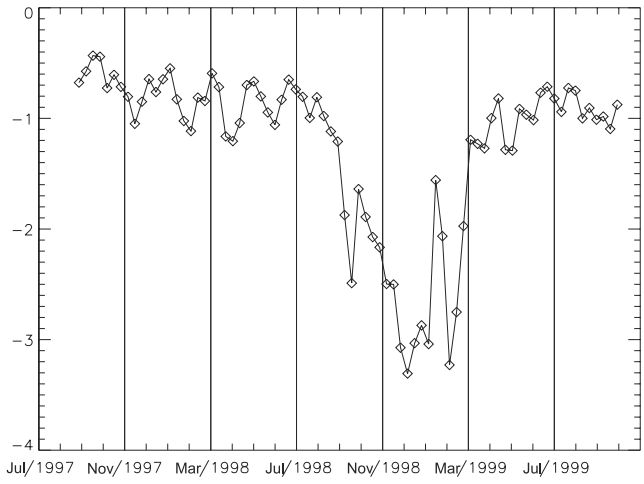

Figure 16. Time evolution of the minimum geostrophic relative vorticity observed in the Balearic Sea. Vorticity was computed from SLA maps covering the same domain as Figure 8. Units are 10^{-5} s^{-1}.

Table 1. Temporal Distribution of the Data Represented in Figure 7

	AVHRR	T/P Track
a	13 Oct. 1998	16 Oct. 1998
b	09 Nov. 1998	...
c	13 Dec. 1998	14 Dec. 1998
d	05 Jan. 1999	03 Jan. 1999
e	15 Jan. 1999	13 Jan. 1999
f	24 Jan. 1999	23 Jan. 1999
g	05 Feb. 1999	02 Feb. 1999
h	25 Feb. 1999	21 Feb. 1999
i	02 March 1999	03 March 1999

ment showed that wind forcing would produce by itself a strong inflow of recent AW through the Mallorca channel.

[45] The second key aspect to be considered is the anomalous path followed by recent AW once it passed through the channels: instead of flowing close to the Balearic Islands (i.e., feeding the Balearic current), it seems that it may have crossed the basin and reached the Catalan coast. During the MEDIPROD-5 experiment, *Millot* [1991] observed similar displacements of a surface drifter that crossed the Mallorca channel and then deviated northwestward, more or less perpendicularly to the Northern current. Although this could be due to a current very close to the surface, also the numerical experiments of *Herbaut et al.* [1997] showed that the wind forcing alone would produce a similar flow path. An important consequence of this anomalous path is that recent AW can flow northward along the Catalan coast and reach the region of influence of Mistral winds.

[46] Therefore, the observed path of AW could be due either to an enhancement of the wind regime or to an anomalous weakening of the Northern current. A preliminary analysis of meteorological data did not reveal any significant departure from climatology, so that the second hypothesis seems more likely. Regarding the causes of this weakening, they could be related not only to regional forcing, but also to remote forcing acting on the Mediterranean general circulation. An exploratory work aimed to determine these ultimate mechanisms should be based mainly on numerical simulations, and it is therefore out of the scope of this study.

[47] Finally, the third key point is the generation of anticyclonic vorticity by wind stress curl. According to the theory of wind-driven circulation (Sverdrup balance [*Pedlosky*, 1987]) and the climatological distribution of wind stress curl in the Mediterranean [e.g., *Hellerman and Rosenstein*, 1983], the northwesterly Mistral jet would produce cyclonic vorticity over the Gulf of Lions and anticyclonic vorticity over the Balearic Basin. This is confirmed by the work by *Herbaut et al.* [1997, Figure 21], which shows that the isolated effect of the wind would yield the formation of a strong anticyclonic eddy in the middle of the Balearic Sea. Moreover, the size of the eddy produced by the simulations ($\sim$100 km diameter), its position (centered at about 40.5°N and 3.5°E) and intensity (velocities of about 50 cm/s) are very similar to those inferred from altimetry and SST images in the present work.

[48] On the other hand, in the numerical experiments by *Pinardi and Navarra* [1993], which include the density driven circulation, the anticyclonic vorticity over the Balearic Basin is much weaker and not located in the middle of the basin, but on the eastern flank of Menorca (an apparently wind-induced anticyclonic eddy observed in that position is mentioned by *Fuda et al.* [2000]). This suggests that the cyclonic thermohaline circulation dominating the region plays a key role inhibiting the generation of anticyclonic vorticity in the Balearic Sea. This would explain the common assumption that the wind-driven circulation in the Balearic Sea consists of small-scale transient features superimposed onto the dominant thermohaline circulation [e.g., *García-Ladona et al*, 1994].

[49] Figure 16 shows that after the eddy was formed (by middle September), the pool of negative relative vorticity continued deepening for three months (an absolute minimum of $-3.5 \cdot 10^{-5}$ s^{-1} was reached in December). The intensification during this 3 month period could be explained in terms of a more or less continuous transference of vorticity from the dominant Mistral winds, but also in terms of conservation of potential vorticity or of a combination of the two. Thus, relative vorticity could have become more negative at the expenses of a vertical compression of the eddy (e.g. due to the intrusion of intermediate/deep water masses underneath the recent AW). However, neither satellite (surface) data nor the data from a single oceanographic cruise (reporting no temporal evolution) allow to investigate these hypotheses. Finally, another mechanism that could have contributed to reinforce the system is the feeding of the eddy with recent AW coming straight from the Ibiza or Mallorca channels (observed in Figure 7, in November).

[50] Concerning the disappearance of the eddy, it was first distorted (in January) by a cold water jet producing a reduction of its negative relative vorticity, and in February it seems that it started to debilitate. Although part of the apparent weakening could be due to the displacement of the eddy with respect to the T/P track, the strengthening of the Northern current, apparent from AVHRR images, is probably relevant. The dominant density-driven circulation would have started to inhibit again the generation of anticyclonic vorticity over the Balearic Basin, then cutting the main source of vorticity of the eddy. From this moment, a few weeks would have been enough for the eddy to decay by frictional effects, since no signature of the eddy is apparent in the satellite data by the middle of March.

[51] **Acknowledgments.** We acknowledge all the participants of the cruise *Hivern-99* (specially the cruise leaders: Marta Estrada and Jordi Salat). We thank Emma D'Acunzo for the AVHRR image processing; Dr Rosalia Santoleri, Dr Jean-Michel Pinot and Dr Simón Ruiz for their useful suggestions on the contents and presentation of this work. We are also grateful to Joan Campins, who kindly revised the meteorological situation during August–September 1998. Ananda Pascual holds a doctoral fellowship from the Universitat de les Illes Balears. Bruno Buongiorno Nardelli activity has been funded by ARS-00-21 contract of the Agenzia Spaziale Italiana.The altimetric data were produced by Collecte Localisation Satellites (Toulouse, France) as part of the MATER project. The AVHRR images were acquired and processed by Istituto di Fisica dell'Atmosfera (Rome, Italy). The meteorological maps come from the HIRLAM-INM model, provided by Instituto Nacional de Meteorología (Spain). The oceanographic cruise *Hivern-99* was funded by the Spanish CICYT project, MAR98-0932. Finally, we want to thank the two anonymous reviewers, whose comments have definitely contributed to increase the quality of this manuscript.

References

Benzohra, M., and C. Millot, Hydrodynamics of an open sea Algerian eddy, *Deep Sea Res., Part I*, *42*, 1831–1847, 1995.

Buongiorno Nardelli, B., R. Santoleri, D. Iudicone, S. Zoffoli, and S. Mar-

ullo, Altimetric signal and three-dimensional structure of the sea in the Channel of Sicily, *J. Geophys. Res.*, *104*, 20,585–20,603, 1999.
Font, J., J. Salat, and J. Tintoré, Permanent features of the circulation in the Catalan Sea, *Oceanol. Acta*, *11*, 51–57, 1988.
Font, J., E. García-Ladona, and E. G. Gorriz, The seasonality of mesoscale motion in the Northern current of the western Mediterranean: Several years of evidence, *Oceanol. Acta*, *18*, 207–219, 1995.
Fuda, J. L., C. Millot, I. Taupier-Letage, U. Send, and J. M. Bocognano, XBT monitoring of a meridian section across the western Mediterranean Sea, *Deep Sea Res., Part I*, *47*, 2191–2218, 2000.
García-Ladona, E., J. Tintoré, J. M. Pinot, J. Font, and M. Manriquez, Surface circulation and dynamics of the Balearic Sea, in *Seasonal and Interannual Variability of the Western Mediterranean Sea, Coastal Estuarine Stud.*, vol. 46, edited by P. E. La Violette, pp. 73–91, AGU, Washington, D. C., 1994.
Gilson, J., D. Roemmich, B. Cornuelle, and L.-L. Fu, Relation of TOPEX/Poseidon altimetric height to steric height and circulation in the North Pacific, *J. Geophys. Res.*, *103*, 27,947–27,965, 1998.
Gomis, D., S. Ruiz, and M. A. Pedder, Diagnostic analysis of the 3D ageostrophic circulation from a multivariate spatial interpolation of CTD and ADCP data, *Deep Sea Res., Part I*, *48*, 269–295, 2001.
Hellerman, S., and M. Rosenstein, Normal wind stress over the world ocean with error estimates, *J. Phys. Oceanogr.*, *13*, 1093–1104, 1983.
Herbaut, C., F. Martel, and M. Crépon, A sensitivity study of the general circulation of the western Mediterranean Sea, part II, The response to atmospheric forcing, *J. Phys. Oceanogr.*, *27*, 2126–2145, 1997.
Horton, C., J. Kerling, G. Athey, J. Schmitz, and M. Clifford, Airborne expendable bathythermograph surveys of the eastern Mediterranean, *J. Geophys. Res.*, *99*, 9891–9905, 1994.
Laing, A. K., and P. G. Challenor, Estimation of mean dynamic height from altimeter profiles and hydrography, *J. Atmos. Oceanic. Technol.*, *16*, 1873–1879, 1999.
Larnicol, G., N. Ayoub, and P. Y. Le Traon, Major changes in Mediterranean Sea level variability from seven years of TOPEX/Poseidon and ERS-1/2 data, *J. Mar. Syst.*, *33–34*, 63–89, 2002.
La Violette, P. E., J. Tintoré, and J. Font, The surface circulation of the Balearic Sea, *J. Geophys. Res.*, *95*, 1559–1568, 1990.
Le Traon, P.-Y., and F. Ogor, ERS-1/2 orbit improvement using TOPEX/Poseidon: The 2 cm challenge, *J. Geophys. Res.*, *103*, 8045–8057, 1998.
Le Traon, P.-Y., F. Nadal, and N. Ducet, An improved mapping method of multi-satellite altimeter data, *J. Atmos. Oceanic Technol.*, *15*, 522–534, 1998.
López García, M. J., C. Millot, J. Font, and E. García-Ladona, Surface circulation variability in the Balearic Basin, *J. Geophys. Res.*, *99*, 3285–3296, 1994.
López-Jurado, J. L., J. García-Lafuente, J. M. Pinot, and A. Álvarez, Water exchanges in the Balearic Islands, *Bull. Inst. Oceanogr.*, *17*, 41–63, 1996.
MacClain, E. P., W. G. Pichel, and C. C. Walton, Comparative performance of AVHRR-based multichannel sea surface temperatures, *J. Geophys. Res.*, *90*, 11,587–11,601, 1985.
MEDOC Group, Observation of formation of deep water in the Mediterranean Sea in 1969, *Nature*, *227*, 1037–1040, 1970.
Melander, M. V., J. C. McWilliams, and N. J. Zabusky, Axisymmetrization and vorticity-gradient intensification on isolated two-dimensional vortex through filamentation, *J. Fluid Mech.*, *178*, 137–159, 1987.
Millot, C., Mesoscale and seasonal variabilities of the circulation in the western Mediterranean, *Dyn. Atmos. Oceans*, *15*, 179–214, 1991.
Millot, C., Circulation in the western Mediterranean Sea, *J. Mar. Syst.*, *20*, 423–442, 1999.
Pedlosky, J., *Geophysical Fluid Dynamics*, 2nd ed., Springer-Verlag, New York, 1987.
Pinardi, N., and A. Navarra, Baroclinic wind adjustment processes in the Mediterranean Sea, *Deep Sea Res., Part II*, *40*, 1299–1326, 1993.
Pinot, J. M., J. Tintoré, and D. Gomis, Quasi-synoptic mesoscale variability in the Balearic Sea, *Deep Sea Res., Part I*, *41*, 897–914, 1994.
Pinot, J. M., J. Tintoré, and D. Gomis, Multivariate analysis of the surface circulation in the Balearic Sea, *Prog. Oceanogr.*, *36*, 343–376, 1995.
Pinot, J. M., J. L. López-Jurado, and M. Riera, The CANALES experiment (1996–98): Interanual, seasonal, and mesoscale variability of the circulation in the Balearic Channels, *Prog. Oceanogr.*, in press, 2002.
Puillat, I., I. Taupier-Letage, and C. Millot, Algerian eddies lifetimes can near 3 years, *J. Mar. Syst.*, *31*, 245–259, 2002.
Ruiz, S., J. Font, M. Emelianov, J. Isern-Fontanet, C. Millot, J. Salas, and I. Taupier-Letage, Deep structure of an open sea eddy in the Algerian Basin, *J. Mar. Syst.*, *33–34*, 179–195, 2002.
Tapley, B. D., et al., Precision orbit determination for TOPEX/Poseidon, *J. Geophys. Res.*, *99*, 24,383–24,404, 1994.
Tintoré, J., D. P. Wang, and P. E. La Violette, Eddies and thermohaline intrusions of the shelf/slope front off the northeast Spanish coast, *J. Geophys. Res.*, *95*, 1627–1633, 1990.

B. Buongiorno Nardelli, Istituto di scienze dell'atmosfera e del climasezine di Roma (CNR), via del fosso del Cavaliere 100, 00133 Roma, Italy.
M. Emelianov, Centre Mediterrani d'Investigacions Marines i Ambientals, CMIMA, (CSIC), Passeig Maritim de la Barceloneta 37–49, 08003 Barcelona, Spain.
D. Gomis and A. Pascual, Institut Mediterrani d'Estuidis Avançats, IMEDEA (CSIC-UIB), C/Miquel Marquès 21, 07190 Esporles, Mallorca, Spain. (ananda.pascual@uib.es)
G. Larnicol, CLS Space Oceanography Division, 8–10 Rue Hermès, 31526 Ramonville St. Agne, France.

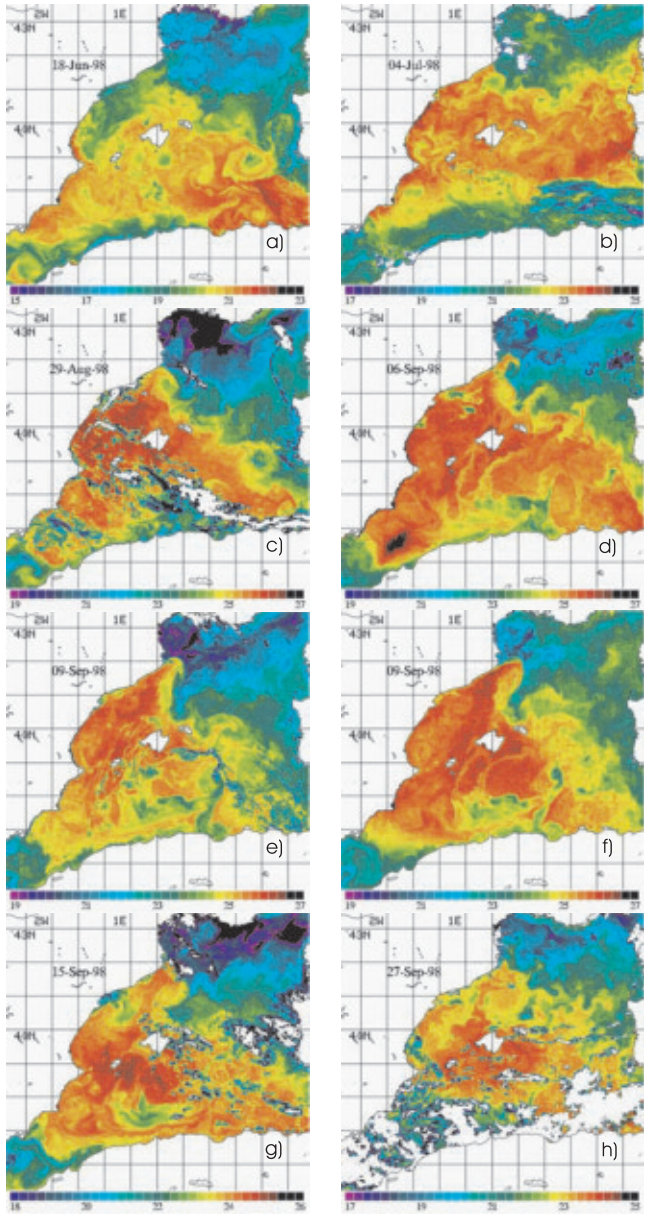

Figure 4. Sequence of AVHRR images of the western Mediterranean. Longitude labels correspond to the ticks on the left.

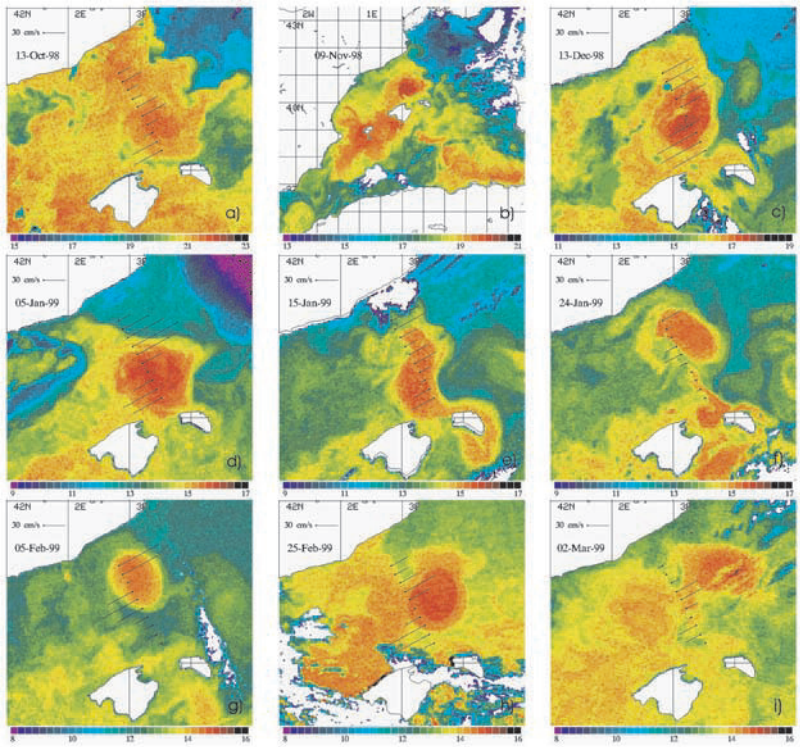

Figure 7. Sequence of AVHRR images of the Balearic Sea. Vectors of cross-track geostrophic velocities inferred from T/P along-track data have been overplotted.

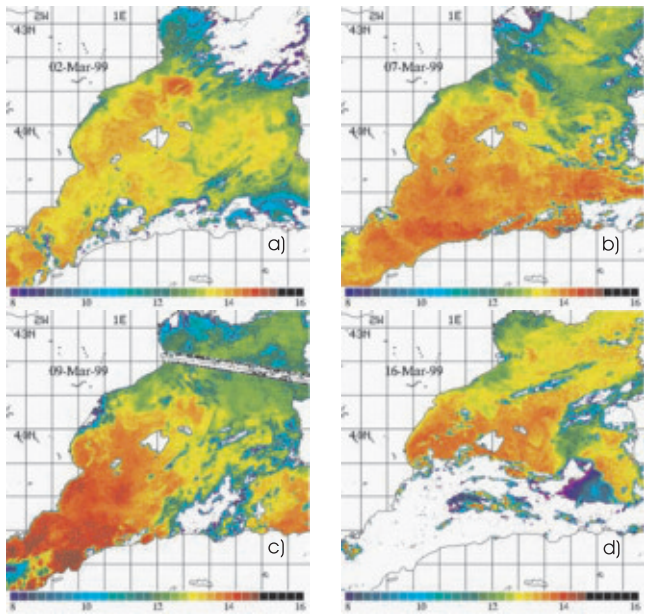

Figure 15. Sequence of AVHRR images of the western Mediterranean. Longitude labels correspond to the ticks on the left.